

# Compatibility Enhancement of ABS/Polycarbonate Blends

D. W. JIN,<sup>1</sup> K. H. SHON,<sup>1</sup> H. M. JEONG,<sup>2</sup> B. K. KIM<sup>3</sup>

<sup>1</sup> Hyosung-BASF, R & D Team, 472-1, Sanggae Dong, Ulsan, Korea

<sup>2</sup> Department of Chemistry, University of Ulsan, Ulsan 680-749, Korea

<sup>3</sup> Department of Polymer Science and Engineering, Pusan National University, Pusan 609-735, Korea

Received 18 November 1996; accepted 27 December 1997

**ABSTRACT:** The effects of blend composition, melt viscosity of poly(acrylonitrile-butadiene-styrene) (ABS), and compatibilizing effect of poly(methyl methacrylate) (PMMA) on mechanical properties of ABS/polycarbonate (PC) blends at ABS-rich compositions were studied. As the content of PC was increased, impact strength and Vicat softening temperature (VST) were increased. As the melt viscosity of ABS was increased near to that of PC, finer distribution of dispersed PC phase and consequent enhanced impact strength and VST were observed. The compatibilizing effect of PMMA can be ascertained from the enhanced properties of  $\frac{1}{4}$ -inch notch impact strength, VST, tensile strength, and the morphology observed by a scanning electron microscope. The improved adhesion of the ABS/PC interface by PMMA changed the fracture mechanism and reduced the notch sensitivity of blends. © 1998 John Wiley & Sons, Inc. *J Appl Polym Sci* 69: 533–542, 1998

**Key words:** ABS; polycarbonate; poly(methyl methacrylate); compatibilizer; morphology; impact strength

## INTRODUCTION

The morphology that determines the physical properties of immiscible polymer blends can be controlled by rheological and thermodynamic factors.<sup>1</sup>

A fine and uniform distribution of the minor component in the major one is generally observed when the melt viscosities of the components are similar.<sup>2</sup> The phase inversion generally occurs at the composition where the higher melt viscosity component is richer, because the component with lower melt viscosity is more prone to be the continuous phase at balanced composition.<sup>3,4</sup>

Homopolymers, as well as a block or graft copolymer, can be used as compatibilizers that act as

interfacial agents, reducing the interfacial tension and promoting the adhesion at the interface.<sup>5</sup>

It was reported that the poly(methyl methacrylate) (PMMA) located at the interface of polycarbonate (PC) and poly(styrene-co-acrylonitrile) (AN) (SAN) contained 31 wt % of AN.<sup>6</sup> We observed the compatibilizing effect of PMMA in a  $\frac{1}{4}$ -inch blends when the AN content of SAN in ABS was 35 wt %, <sup>7</sup> and impact strength of poly(AN-butadiene-styrene) (ABS)/PC notch specimen was enhanced in the presence of PMMA. However in some specimens, we observed that a  $\frac{1}{8}$ -inch notch impact strength was decreased when compatibilized with PMMA, although a  $\frac{1}{4}$ -inch notch impact strength was increased.

To explain this abnormal result, in the present study, we observed the fractured surface of ABS/PC blends to examine the effect of ABS properties and PMMA on the fracturing mechanism of the blends at ABS-rich compositions.

Correspondence to: K. H. Shon.

*Journal of Applied Polymer Science*, Vol. 69, 533–542 (1998)  
© 1998 John Wiley & Sons, Inc. CCC 0021-8995/98/030533-10

**Table I** Characteristics of Polymers Used in This Study

Resin Notation	Weight-Average Molecular Weight	Number-Average Molecular Weight	Melt Index <sup>a</sup> (mL 10 min <sup>-1</sup> )	Polybutadiene Rubber Content in ABS (wt %)	Average AN Content in SAN (wt %)
PC	22,800	9,760	—	—	—
PMMA	66,000	35,000	—	—	—
ABS-1	—	—	13	18	35
ABS-2	—	—	5	18	35
ABS-3	—	—	3	18	35
ABS-4	—	—	40	6	35
ABS-5	—	—	25	12	35
ABS-6	—	—	5	24	35

<sup>a</sup> Measured at 220°C with a 10-kg load.

Some observed results and suggested energy absorption mechanism during fracturing are reported in this article.

## EXPERIMENTAL

Commercial grade of resins, with the physicochemical properties listed in Table I, were used as received. The ABS's were produced by Hyosung BASF and consist of SAN and SAN-grafted polybutadiene latex rubber. The amount of rubber in ABS was adjusted by the relative amount of SAN and a SAN-grafted polybutadiene. The particles of polybutadiene rubber range in size from 0.1 to 0.4  $\mu\text{m}$ . The melt index of ABS at a fixed amount of rubber was adjusted by the melt index of constituent SAN. The melt viscosity of polymer measured with a capillary rheometer (Goeffert 2002) at 240°C at various shear rates is shown in Figure 1.

Dried resins for 2 h at 80°C in vacuum were hand-mixed thoroughly at proper compositions, followed by melt blending using a corotating twin-screw extruder (Berstorff ZE 25, L/D = 33) at a zone temperature profile of 240–270°C and 300 rpm. Extrudates were quenched in water and pelletized. Injection molding was done at a temperature similar to that of blending.

Notched Izod impact strength, Vicat softening temperature, and tensile strength of the injection-molded specimen were determined according to the standard procedures described in ASTM D256, D1525, and D638.

After measurement of Izod impact strength at room temperature, the morphology of fractured surface was observed using a scanning electron microscope (SEM; Jeol JSM820).

## RESULTS AND DISCUSSION

### Morphology

The overall morphologies of fractured surfaces of ABS/PC (70/30, w/w) blends with a  $\frac{1}{4}$ -inch notch are shown in Figure 2. The stress whitening was observed at the edge and at the parabolic beach marks. The stress-whitened area was <10% of fractured surface in the ABS-1/PC blend. However, the spacing between beach marks decreased and the fraction of the stress-whitened area increased to the order of ABS-1 < ABS-2 < ABS-3 blend. The stress-whitened area was about 30–40% of ABS-2/PC blends and 70–80% for the

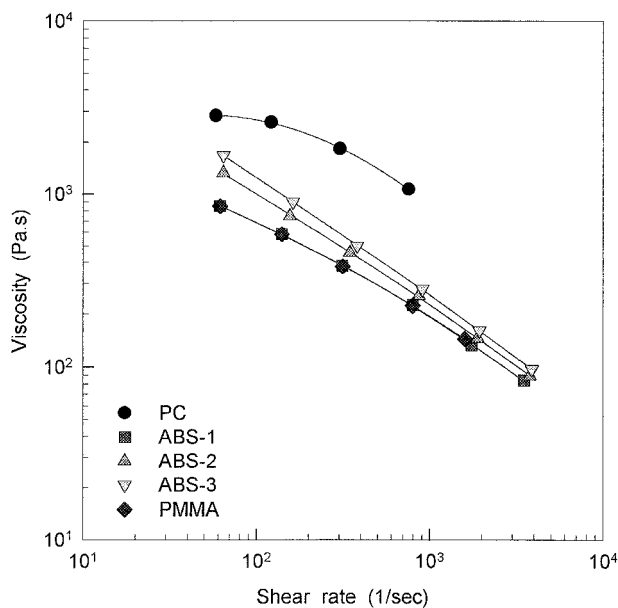
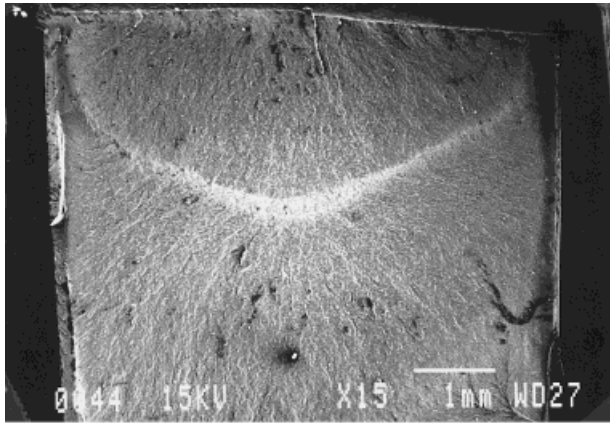
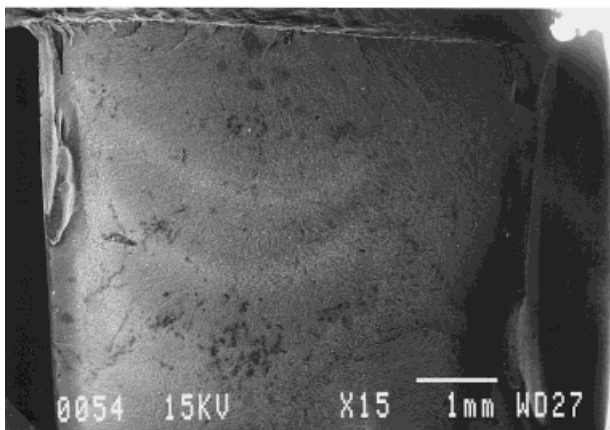


**Figure 1** Melt viscosity of PC, ABS-1, ABS-2, ABS-3, and PMMA at 240°C.



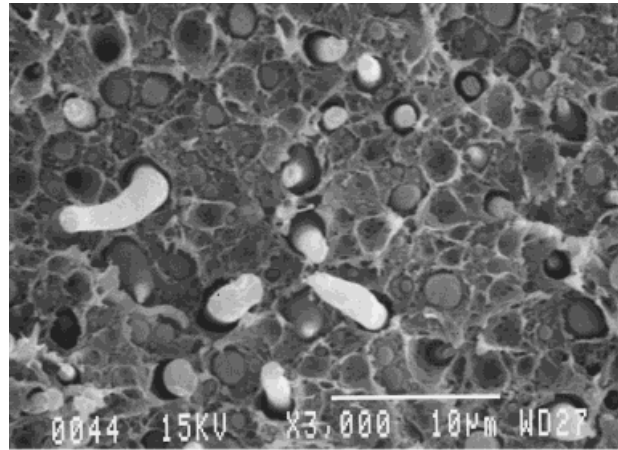
(a)



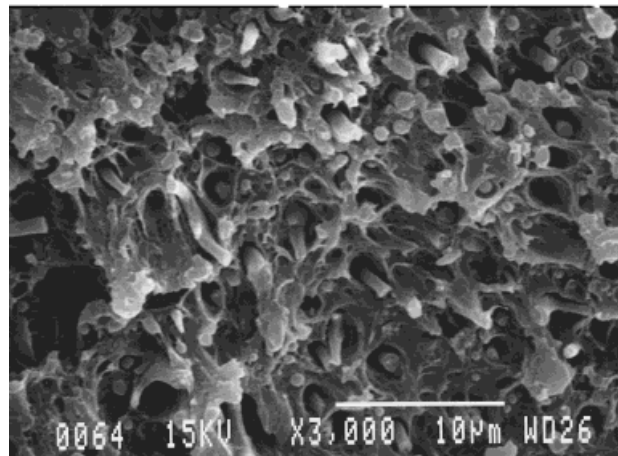
(b)

**Figure 2** SEM micrographs of ABS/PC (70/30, w/w) blends with a  $\frac{1}{4}$ -inch notch and fractured at room temperature: (a) ABS-1/PC and (b) ABS-2/PC.

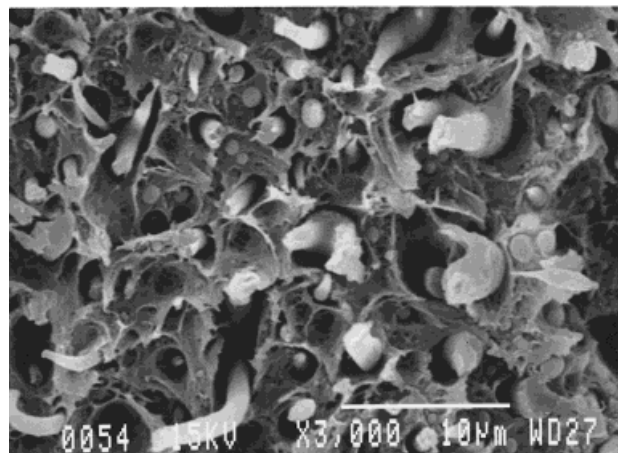
ABS-3/PC blend. The detailed morphologies of fractured surfaces with stress whitening are shown in Figure 3, and those without stress whitening are shown in Figure 4. The surfaces without stress whitening show no deformation of dispersed PC phase or ABS matrix phase, suggesting brittle fracture. However, stress-whitened areas show the plastic deformation of both the dispersed PC phase and ABS matrix phase, with clear separation of the ABS/PC interface. In Figures 3 and 4, we can observe that the size of the dispersed



(a)

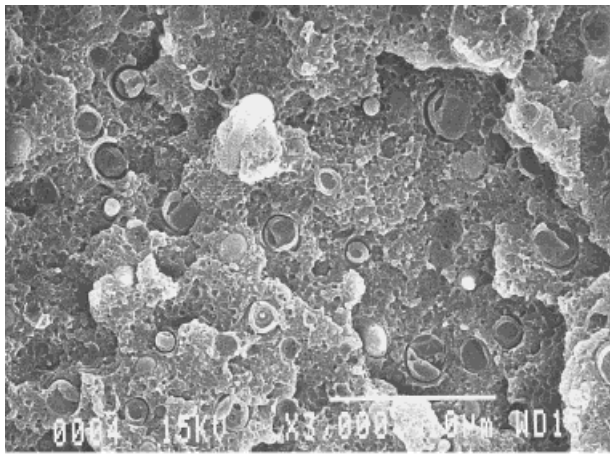


(b)

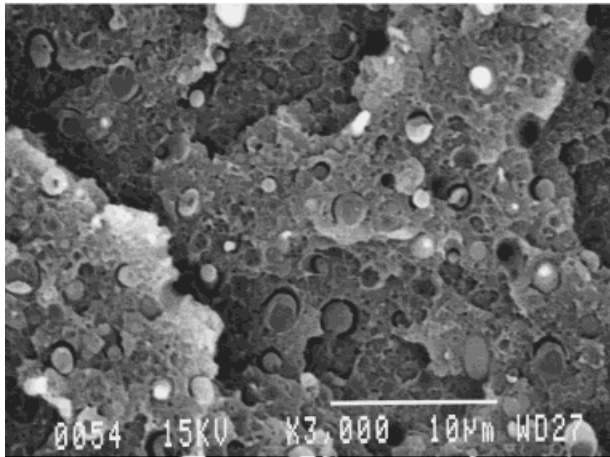


(c)

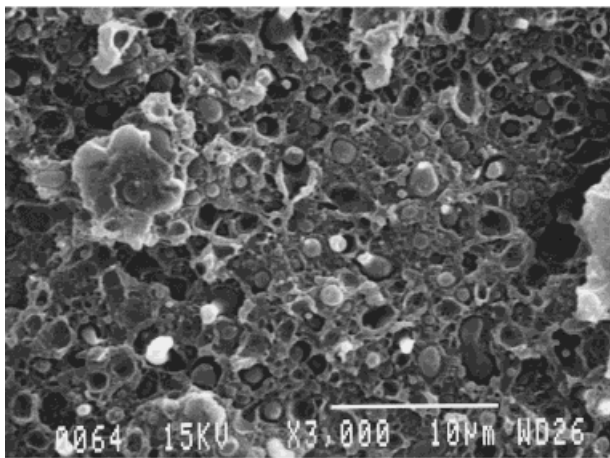
**Figure 3** SEM micrographs of stress-whitened surfaces of ABS/PC (70/30, w/w) blends with a  $\frac{1}{4}$ -inch notch and fractured at room temperature: (a) ABS-1/PC, (b) ABS-2/PC, and (c) ABS-3/PC.



(a)



(b)



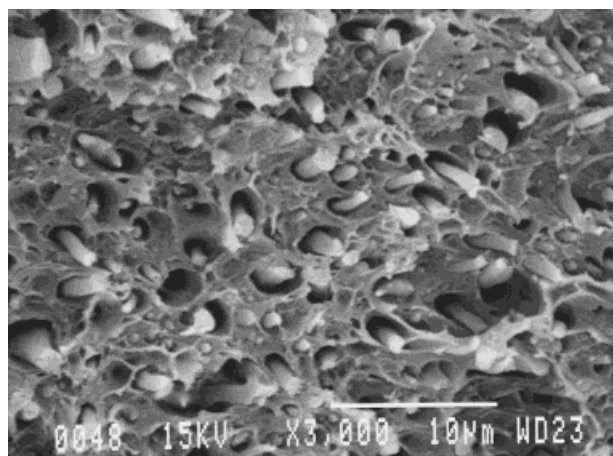
(c)

**Figure 4** SEM micrographs of surfaces without stress whitening of ABS/PC (70/30, w/w) blends with a  $\frac{1}{4}$ -inch notch and fractured at room temperature: (a) ABS-1/PC, (b) ABS-2/PC, and (c) ABS-3/PC.

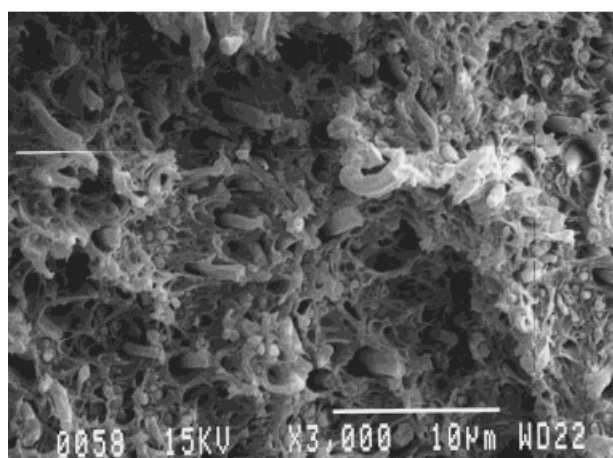
PC phase decreases to the order of ABS-1 > ABS-2 > ABS-3 blend, as the melt viscosity of ABS approaches that of PC, as anticipated.<sup>1,2</sup> The degree of deformation of the dispersed PC phase and matrix ABS phase increases with reverse order. The deformation of thin specimen can be approximated by the plane stress state, whereas a thick specimen is mostly in a plane strain state.<sup>8,9</sup> The stress at which a material yields is greater in a plane strain state than in a plane stress state. Thus, in a plane stress state, a more extensive degree of plasticity develops at the crack tip. So, the above results suggest that the surface created by the debonding of poorly adhered ABS/PC interface seems to reduce thickness effect at microscopic level and to promote ductile fracture, more evidently at a finer dispersion of the minor phase.<sup>9</sup> In the specimen with a  $\frac{1}{8}$ -inch notch (Fig. 5), the fraction of the stress-whitened area and the degree of deformation of both the dispersed phase and matrix phase were increased, compared with that with a  $\frac{1}{4}$ -inch notch (Fig. 3), probably due to the thickness effect. The size of the dispersed PC phase is much smaller in a  $\frac{1}{8}$ -inch notch specimen (Fig. 5), compared with that in a  $\frac{1}{4}$ -inch notch specimen (Fig. 3). This seems to be due to high shear rate during injection molding and rapid cooling rate after injection of a thin  $\frac{1}{8}$ -inch notch specimen. This finer dispersion also seems to be the cause of enhanced deformation during fracturing, compared with that of a  $\frac{1}{4}$ -inch notch specimen, in addition to the thickness effect.

Figure 6 shows the morphology of ABS/PC (70/30, w/w) blends compatibilized with 5 ph of PMMA. No clear ABS/PC interface shows the compatibilizing effect of PMMA.<sup>6,7</sup> All of the fractured surfaces of compatibilized blends were stress-whitened, and the surfaces were more smooth and regular than those of uncompatibilized blends. In the compatibilized blends, it is anticipated that enhanced adhesion between the matrix ABS and dispersed PC phase encourages the cavitation of the low modulus rubber particles and the craze formation of SAN rather than the separation of the ABS/PC interface at the initial stage of deformation.<sup>9,10</sup> This seems to be the cause of uniform stress whitening.

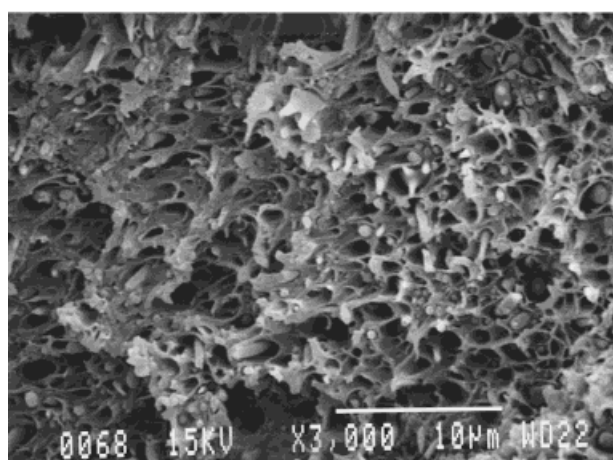
In Figure 7, when the composition of ABS/PC is 55/45 (w/w), we can observe that the size of the dispersed PC phase was increased, compared with the 70/30 blend, and the cocontinuous morphology begins to develop as the melt viscosity of ABS approaches that of PC.<sup>3,4</sup> The stress whitening



(a)

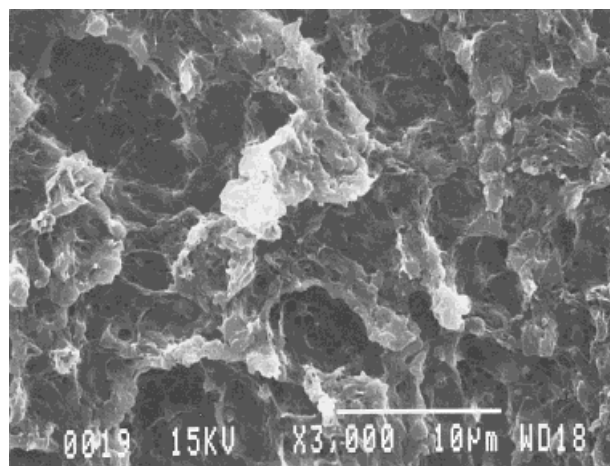


(b)

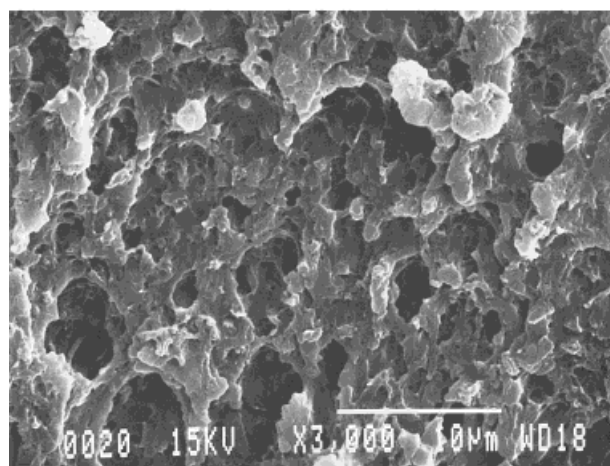


(c)

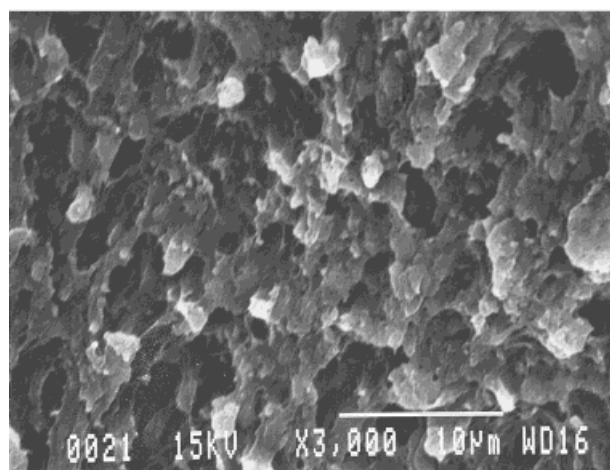
**Figure 5** SEM micrographs of stress-whitened surfaces of ABS/PC (70/30, w/w) blends with a  $\frac{1}{8}$ -inch notch and fractured at room temperature: (a) ABS-1/PC, (b) ABS-2/PC, and (c) ABS-3/PC.



(a)

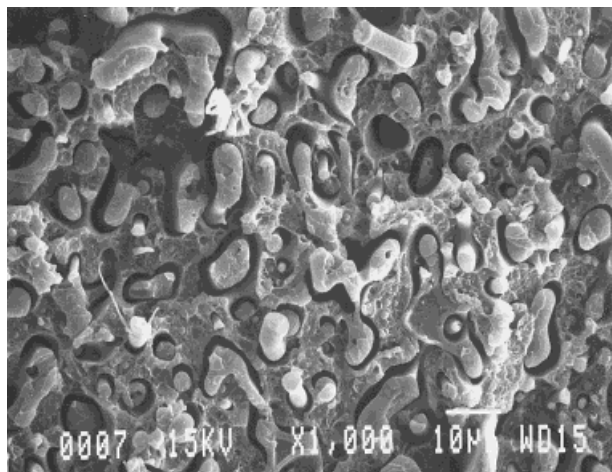


(b)

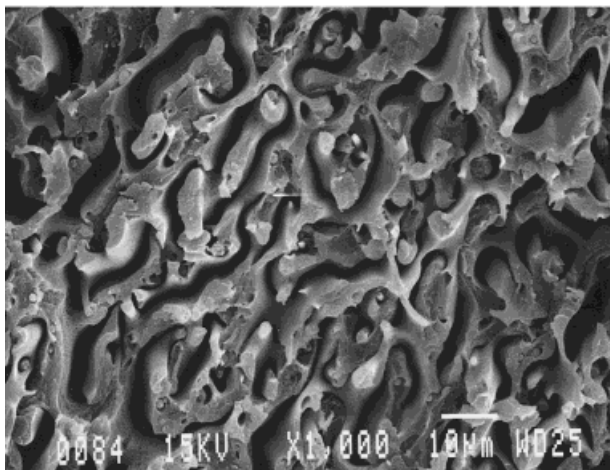


(c)

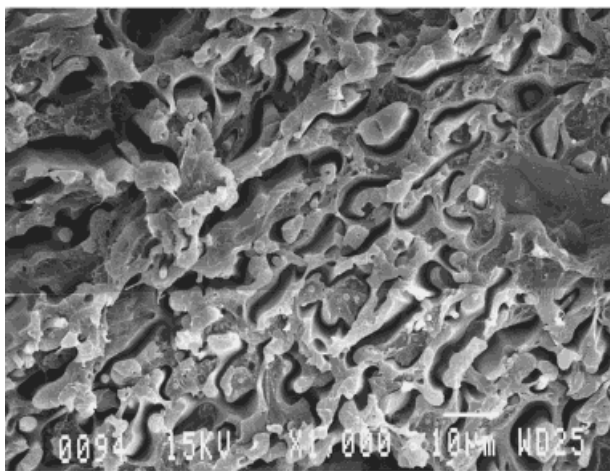
**Figure 6** SEM micrographs of ABS/PC (70/30, w/w) blends compatibilized with 5 ph of PMMA, that have a  $\frac{1}{4}$ -inch notch and were fractured at room temperature: (a) ABS-1/PC, (b) ABS-2/PC, and (c) ABS-3/PC.



(a)



(b)



(c)

**Figure 7** SEM micrographs of stress-whitened surfaces of ABS/PC (55/45, w/w) blends with a  $\frac{1}{4}$ -inch notch and fractured at room temperature: (a) ABS-1/PC, (b) ABS-2/PC, and (c) ABS-3/PC.

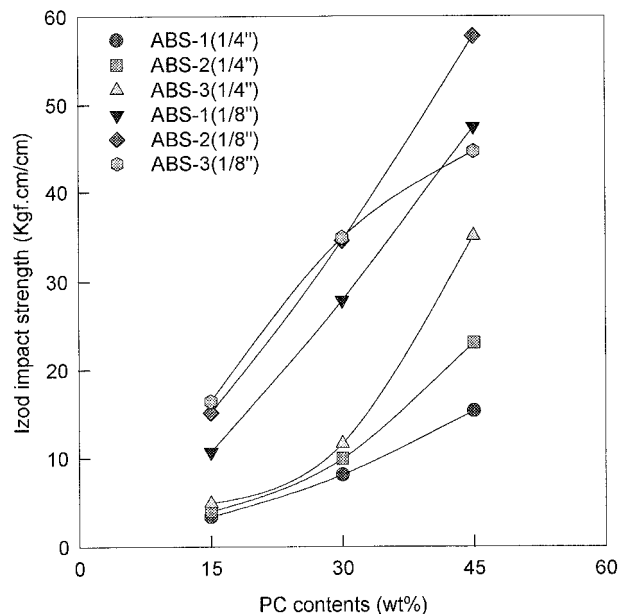


**Figure 8** Izod impact strength of ABS-1, ABS-2, and ABS-3 blends with PC.

ing of 55/45 blends was more obvious than that of 70/30 blends, and the degree of stress whitening increased to the order of ABS-1 < ABS-2 < ABS-3 blend, as in 70/30 blends.

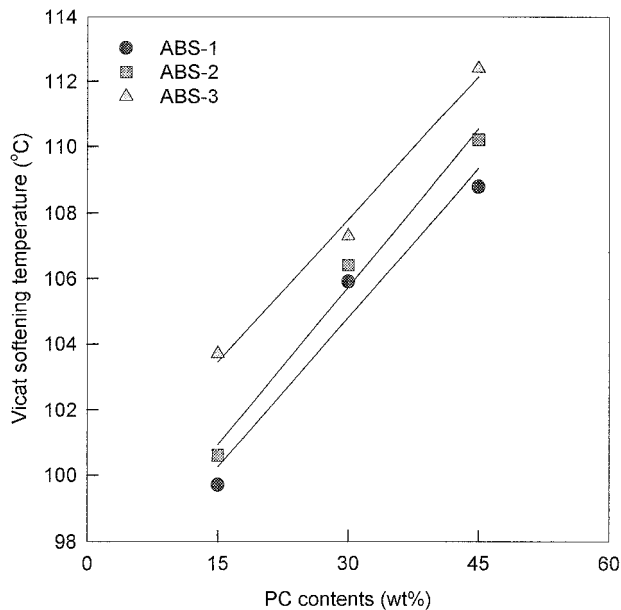
#### Effect of Composition and Melt Viscosity

Figure 8 shows the variation of  $\frac{1}{4}$ -inch and  $\frac{1}{8}$ -inch notch Izod impact strength of ABS/PC blends according to the change of blend composition and melt viscosity of ABS. Enhanced Izod impact strengths are observed as the content of PC and melt viscosity of ABS are increased. The  $\frac{1}{8}$ -inch notch Izod impact strengths are higher than the  $\frac{1}{4}$ -inch notch Izod impact strengths.

If we consider that  $\frac{1}{4}$ -inch notch Izod impact strength of ABS and PC are 20 and 10 Kgf cm  $\text{cm}^{-1}$ , respectively, and  $\frac{1}{8}$ -inch notch Izod impact of ABS and PC are 20 and 80 Kgf cm  $\text{cm}^{-1}$ , respectively, we can see that the values of Izod impact strengths show negative deviations from simple additive rule when the composition of ABS/PC is 85/15 (w/w), and that the values of Izod impact strength lie near the average value of constituent polymers when the composition of ABS/PC is 70/30 (w/w). Similar variation of Izod impact strength according to the blend composition was reported before.<sup>11</sup>

Ductile failure of PC occurs by a shear yielding and brittle failure by crazing, and the predomi-





**Figure 9** VST of ABS-1, ABS-2, and ABS-3 blends with PC.

nant mode is strongly dependent on the thickness of specimen. This is the cause of the difference of  $\frac{1}{4}$ -inch and  $\frac{1}{8}$ -inch notch Izod impact strengths of PC. The ductile failure of ABS is accompanied by the cavitation of rubber particles and craze formation of SAN matrix, thus showing relative insensitivity to specimen thickness.<sup>9,10</sup> In Figures 3 and 5, we observed that the plastic deformation

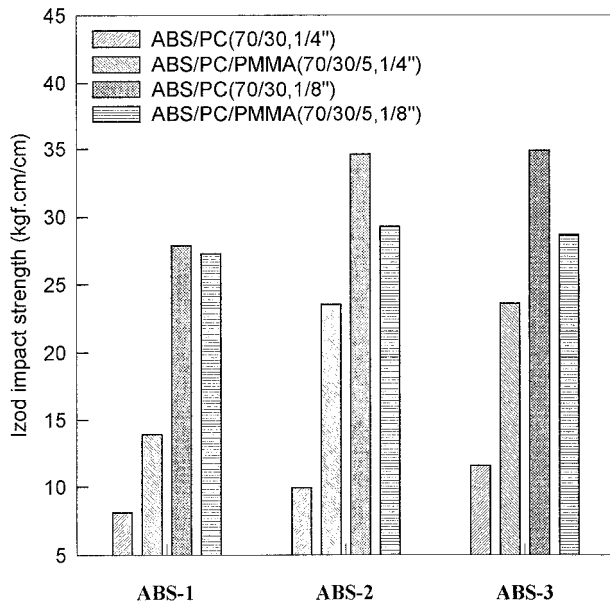


**Figure 10** Izod impact strength of ABS/PC and ABS/PC/PMMA blends.

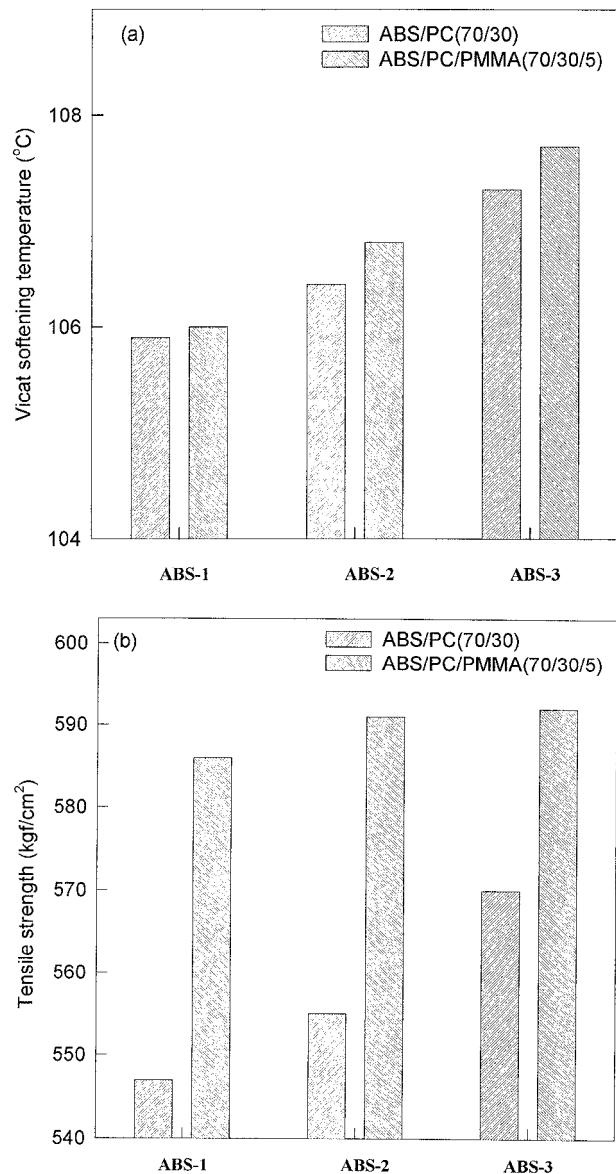


**Figure 11** (a) VST and (b) tensile strength of ABS/PC and ABS/PC/PMMA blends.

of both dispersed PC phase and matrix ABS phase increased as the thickness of specimen was decreased, and the melt viscosity of ABS was increased nearer to that of PC, thus causing finer morphology of the dispersed PC phase. The enhanced plastic deformation of constituent polymers seem to be the cause of enhanced Izod impact strength of a  $\frac{1}{8}$ -inch notch specimen and blends with finely dispersed PC phase.

Figure 9 shows the variation of Vicat softening temperature (VST). Higher values of VST are observed as the content of PC and melt viscosity of ABS are increased. Higher content and better

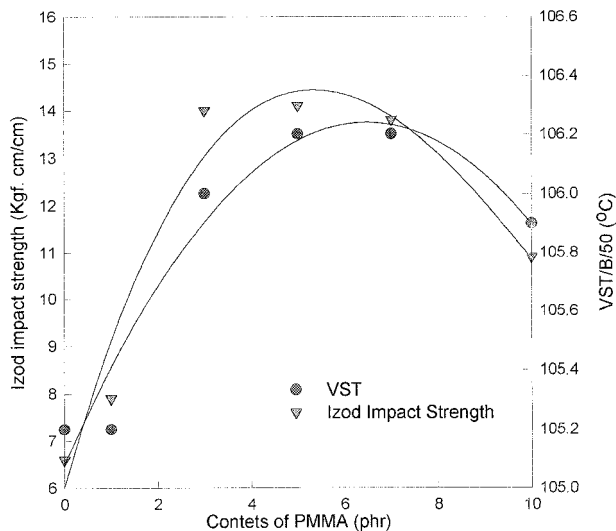


**Figure 12** Izod impact strength and VST of ABS-1/PC (70/30, w/w) blends compatibilized by PMMA.

dispersion of PC, whose value of VST is higher than ABS, seems to be the cause.

#### Compatibilizing Effect of PMMA

In Figure 10, it can be observed that large difference exist between  $\frac{1}{4}$ -inch and  $\frac{1}{8}$ -inch notch Izod impact strengths of uncompatibilized blends,

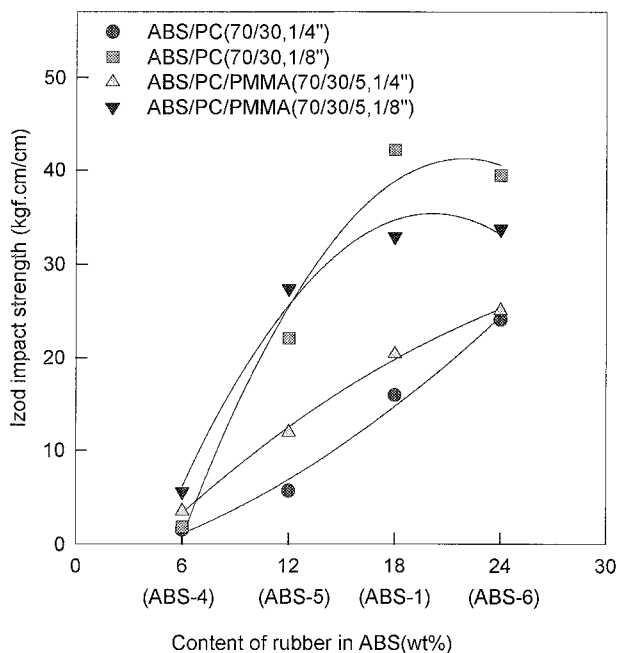
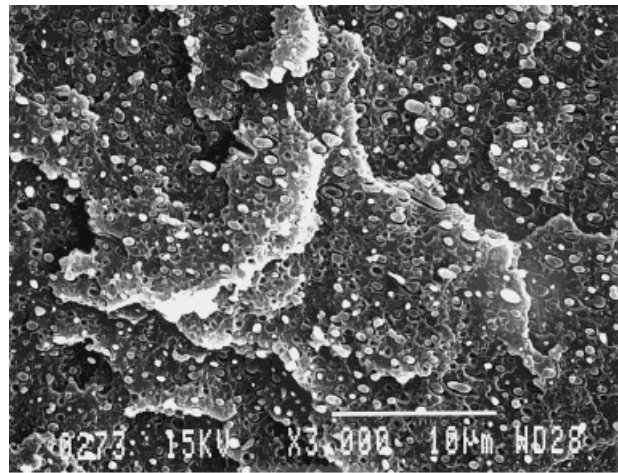
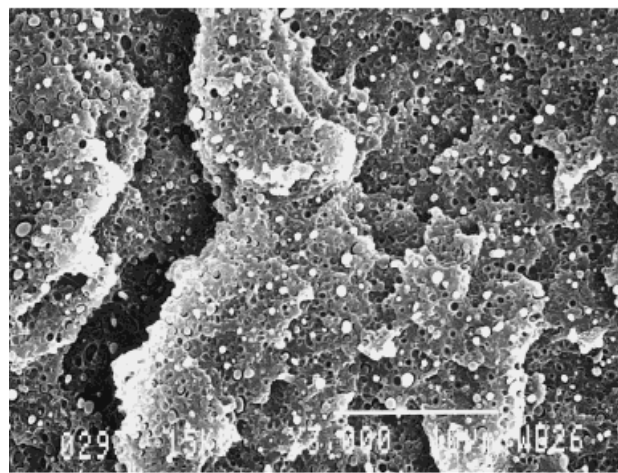


**Figure 13** The  $\frac{1}{4}$ -inch and  $\frac{1}{8}$ -inch notch Izod impact strengths of ABS/PC and ABS/PC/PMMA blends.



(a)

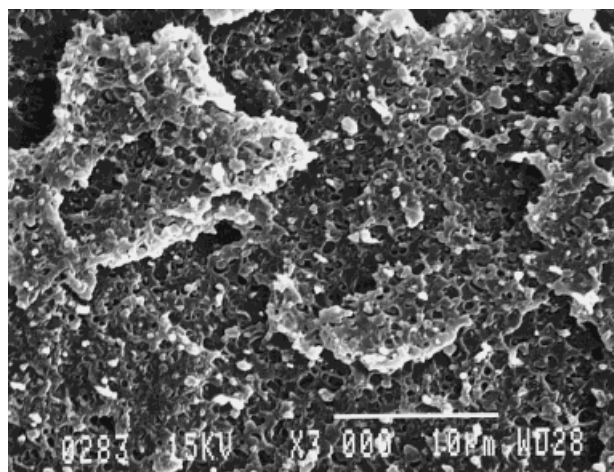


(b)

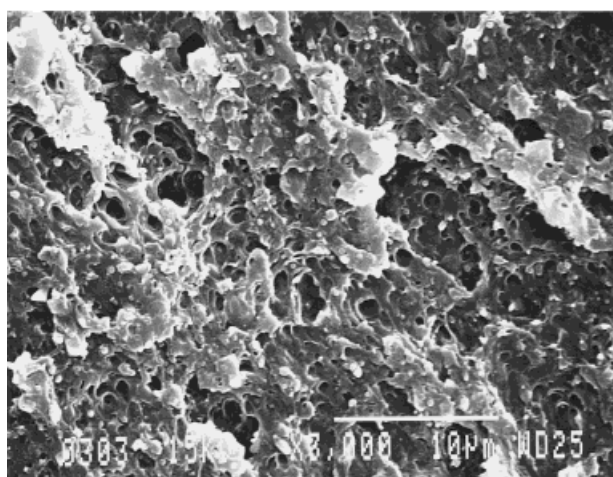
**Figure 14** SEM micrographs of surfaces of ABS/PC (70/30, w/w) blend with a  $\frac{1}{8}$ -inch notch and fractured at room temperature: (a) ABS-4/PC and (b) ABS-5/PC.

whereas this difference is relatively smaller in blends compatibilized by 5 ph of PMMA. The difference of sensitivity on specimen thickness of compatibilized and uncompatibilized blend seems to be due to the difference in fracture mechanism. As explained with Figures 2–5, energy dissipation by plastic deformation of constituent polymer after debonding of poorly adhered interface occurs in the fracture process of uncompatibilized blends. Larger contributions of plastic deformation in a thin specimen (Fig. 5 compared with Figs. 3 and 4) can be illustrated as a cause of enhanced Izod impact strength, compared with a thick specimen. In the compatibilized blends, as





(a)



(b)

**Figure 15** SEM micrographs of surfaces of ABS/PC (70/30, w/w) blends compatibilized with 5 ph of PMMA that have a  $\frac{1}{8}$ -inch notch and were fractured at room temperature: (a) ABS-4/PC and (b) ABS-5/PC.

explained in Fig. 6, the cavitation of rubber particles and the craze formation of SAN contribute as major energy dissipation modes in the fracture process. The relative insensitivity of this mode on specimen thickness, as can be generally observed in ABS, seems to be a cause of relatively insensitive change of Izod impact strength by specimen thickness.<sup>9,11</sup>

In Figure 10, we can also observe that  $\frac{1}{8}$ -inch notch Izod impact strengths of uncompatibilized blends are larger than those of compatibilized blends, whereas  $\frac{1}{4}$ -inch notch Izod impact strength is the reverse. These results show that, for a  $\frac{1}{8}$ -inch notch specimen where plastic deformation in

plane stress state can largely contribute in the energy dissipation because of a finely dispersed PC phase and the thin thickness of the specimen, this energy dissipation after debonding of the ABS/PC interface is more favorable for enhanced Izod impact strength than the energy dissipation by cavitation of rubber or crazing of SAN. They also show that, for a  $\frac{1}{4}$ -inch notch specimen where plastic deformation cannot largely contribute because of the coarsely dispersed PC phase and thick thickness of specimen, energy dissipation by rubber cavitation or SAN crazing is more favorable.

The differences between uncompatibilized and compatibilized blends in the value of Izod impact strength of both  $\frac{1}{4}$ -inch and  $\frac{1}{8}$ -inch notch specimen generally increase to the order of ABS-1 < ABS-2 < ABS-3 blend (Fig. 10). These results suggest the contribution of energy dissipation by plastic deformation in uncompatibilized  $\frac{1}{8}$ -inch notch specimen and the contribution of energy dissipation by rubber cavitation or SAN crazing in compatibilized  $\frac{1}{4}$ -inch notch specimen increase as the degree of intimate mixing increases by melt viscosity match of constituent polymers.

Figure 11 shows that VST and the tensile strength of ABS/PC (70/30, w/w) blends are enhanced by the compatibilizing effect of PMMA.

Figure 12 shows that  $\frac{1}{4}$ -inch notch Izod impact

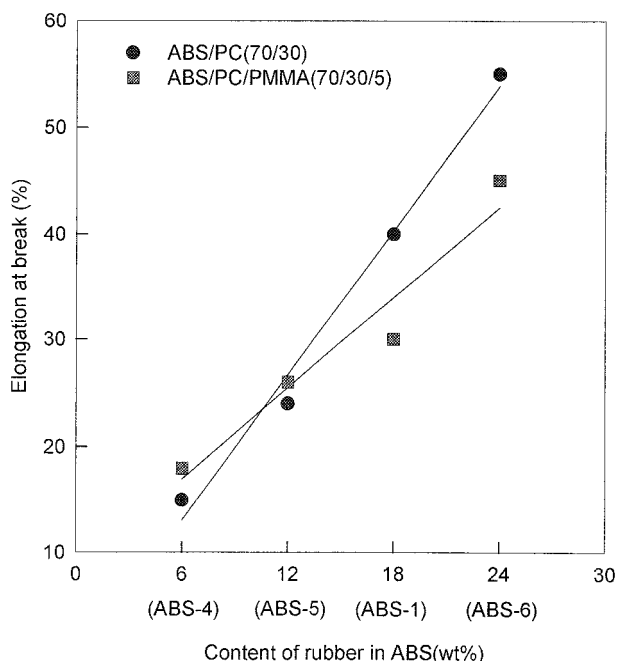


**Figure 16** Elongation at break of ABS/PC and ABS/PC/PMMA blends.

strength and VST increase by compatibilizing effect of PMMA. This effect is saturated at 3 phr of PMMA.

### Effect of Rubber Content

In Figure 13, the relative Izod impact strength value of compatibilized and uncompatibilized blends, a  $\frac{1}{4}$ -inch notch specimen, and a  $\frac{1}{8}$ -inch notch specimen are the same as in Fig. 10 at high polybutadiene rubber content in ABS. However, the relative value of  $\frac{1}{8}$ -inch notch Izod impact strength is reversed at low polybutadiene rubber content. This result suggests insufficient contribution of plastic deformation of a uncompatibilized  $\frac{1}{8}$ -inch notch specimen at low polybutadiene rubber content. This could be ascertained from the fractured surface with almost no stress whitening and SEM micrographs shown in Figure 14. Only minor deformation of the dispersed PC phase and no deformation of the ABS matrix after debonding of the ABS/PC interface due to fracturing can be observed in Figure 14(a,b). Almost all of the fractured surface of ABS-5/PC blend compatibilized with 5 phr of PMMA was stress-whitened, and the deformed and uneven fractured surface shown in Figure 15(b) suggest the ductile fracturing process accompanied by crazing of the ABS matrix. Minor stress whitening and reduced unevenness and deformation of the fractured surface of the ABS-4/PC blend compatibilized by 5 phr of PMMA [Fig. 15(a)] suggest somewhat reduced crazing of the ABS matrix due to low rubber content.

The relatively lower value of elongation at the break of uncompatibilized blends at low polybutadiene rubber content in Figure 16 also suggests a relatively minor contribution of plastic deformation at low polybutadiene rubber content.

## CONCLUSIONS

In our ABS/PC blends of ABS-rich compositions,

1. Izod impact strength and VST were increased as the content of PC in blend was increased from 15 to 45 wt %.
2. When the melt viscosity of ABS was increased nearer to that of PC, finer distribution of the dispersed PC phase and consequent enhanced Izod impact strength and VST were observed.
3. PMMA was effective as a compatibilizer to enhance  $\frac{1}{4}$ -inch notch Izod impact strength, VST, and tensile strength of blends.
4. Improved adhesion of the ABS/PC interface by PMMA seems to change the energy dissipation mechanism in the fracture process.

## REFERENCES

1. S. Wu, *Polym. Eng. Sci.*, **27**, 335 (1987).
2. S. M. Lee, C. H. Choi, and B. K. Kim, *J. Appl. Polym. Sci.*, **51**, 1765 (1994).
3. I. S. Miles and A. Zurek, *Polym. Eng. Sci.*, **28**, 796 (1988).
4. B. K. Kim, M. S. Kim, and K. J. Kim, *J. Appl. Polym. Sci.*, **48**, 1271 (1993).
5. M. E. J. Dekkers, S. Y. Hobbs, and V. H. Watkins, *Polymer*, **32**, 2150 (1991).
6. D. Debier, J. Devaux, R. Legras, and D. Leblanc, *Polym. Eng. Sci.*, **34**, 613 (1994).
7. K. J. Choi, G. H. Lee, S. J. Ahn, K. H. Shon, I. Kim, and H. M. Jeong, *J. Appl. Polym. Sci.*, **59**, 557 (1996).
8. A. J. Kinloch and R. J. Young, *Fracture Behavior of Polymers*, Elsevier, London, 1985.
9. M.-P. Lee, A. Hiltner, and E. Baer, *Polym. Eng. Sci.*, **32**, 909 (1992).
10. H. Goto, K. Kuratani, H. Kito, T. Shimono, and K. Ogura, *Kobunshi Ronbunshu*, **51**, 752 (1994).
11. B. S. Lombardo, H. Keskkula, and D. R. Paul, *J. Appl. Polym. Sci.*, **54**, 1697 (1994).